34th Annual International Conference of the IEEE EMBS
San Diego, California USA, 28 August - 1 September, 2012

An investigation into the viability of image processing for the measurement of sarcomere length in isolated cardiac trabeculae

Alexander J. Anderson, Poul M. F. Nielsen, *Member IEEE*, Andrew J. Taberner, *Member IEEE*

Abstract— **A preliminary investigation was performed into the viability of using frequency domain image processing techniques to determine sarcomere length from bright-field images of isolated cardiac trabecula in real-time. Hardware based data processing was used to compute the average sarcomere length in a cardiac trabecula undergoing stretch. Our technique estimated the increase in mean sarcomere length with increasing muscle length as the trabecula was stretched to and beyond the normal physiological limit of 2.4 µm. The standard error in the mean sarcomere length extracted from each image was typically10 nm.**

I. Introduction

With each beat of the heart, its cells release a brief pulse of calcium, which triggers force development and cell shortening, funded by expenditure of energy with its attendant liberation of heat. The degree of interdependence of the centrally important physiological parameters that underlie cardiac muscle contraction has yet to be fully understood. Part of the reason for this has been the inability to simultaneously and continuously measure these parameters during the cardiac contraction cycle.

Cardiac trabeculae are naturally arising collections of linearly arranged myocytes (~2 mm long, ~100 µm radius) and are often selected for use in studies of cardiac muscle function. We have previously constructed [1-4] the only calorimeter in which it is possible to measure, simultaneously, the force development and rate of heat production [5, 6] (and thereby the energetic efficiency) of isolated continuously superfused rat cardiac trabeculae. Force-length work-loop experiments designed to mimic the pressure-volume loops experienced by the heart *in vivo* can be performed using our apparatus. However, until now we have been unable to measure (or control) in real-time the sarcomere length of the muscle in our instrument.

Sarcomere length in cardiac trabeculae has been determined by laser diffraction [7, 8]. Direct imaging has been shown to be viable for single cardiac myocytes [9]. The laser diffraction method returns information regarding the mean sarcomere length in a small central region of the muscle. The direct imaging approach has the potential benefit of providing more information regarding the degree of inhomogeneity in sarcomere length in failing heart muscle.

In this paper, we describe a custom system that we have developed for measuring, in real-time, the sarcomere length distribution from continuously-acquired brightfield illuminated images of cardiac trabeculae. We describe the computational hardware, software, and mechanical apparatus which allow us to perform these measurements. Our method for extracting sarcomere-length estimates from images is based upon interpolation in the frequency domain. We implement this method in hardware to order to provide deterministic measures of mean sarcomere length at update rates of up to 100 Hz.

II. Methods

A. Imaging System Construction

A custom imaging microscope was constructed using the Qioptiq Microbench system. The optical arrangement (Fig. 1) is standard for brightfield microscopy. It consists of a light-source whose light is captured by a collector lens then passed through an iris and subsequently a condenser lens before striking the experimental preparation. After passing through the preparation, the light is collected by the objective lens (Nikon 40x ELWD Ph2-ADL, NA=0.6) and focused through a standard 200 mm tube onto the camera chip at the other end. The condenser illumination was provided by a fiber-coupled halogen lamp (Fiber-Lite PL-900). This arrangement gave us the freedom to build custom stages to allow motor access, and also freedom to modify the optics for optimum contrast.

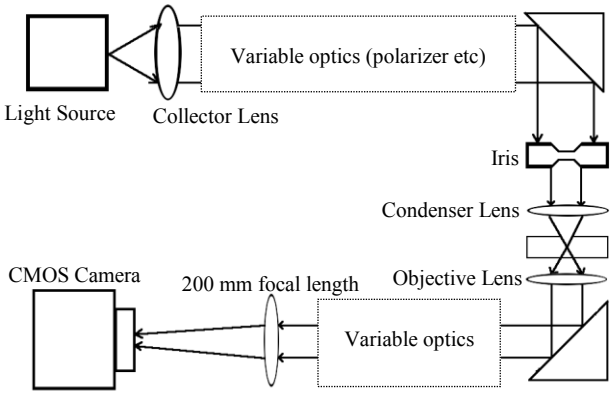

Figure 1: Diagram of OEM microscope optics.

This work was supported by a National Heart Foundation of New Zealand PhD Scholarship, The University of Auckland FRDF and VCSDF grants as well as the Marsden Fund Council from Government funding, administered by the Royal Society of New Zealand (#UOA1108).

A. J. Anderson is with the Auckland Bioengineering Institute, Auckland, New Zealand (phone: +649235102, email: aand063@aucklanduni.ac.nz)

P. M. F. Nielsen is with the Auckland Bioengineering Institute, and the Department of Engineering Science, The University of Auckland, Auckland, New Zealand (email: p.nielsen@auckland.ac.nz)

A. J. Taberner is with the Auckland Bioengineering Institute, and the Department of Engineering Science, The University of Auckland, Auckland, New Zealand (email:a.taberner@auckland.ac.nz).

Sarcomere images were recorded using a 1 Mpixel CMOS camera (Photonfocus MV-D1024E-160CL-12) via Cameralink interface. Image acquisition and processing was performed by a Field Programmable Gate Array (FPGA) card (NI-PXIe 7965R, National Instruments) and CameraLink interface module (NI-1483). Images were acquired from the camera at rates of up to 100 Hz. The FPGA card was mounted in a PXI chassis which is connected to a PC running LabVIEW Real-Time 2011.

B. Supporting Mechanical System

The mechanical system for mounting trabeculae consisted of a miniature Lorentz-force linear motor at one end of the muscle, and a simple fixed attachment hook at the other end (later to be replaced with a force transducer). The motor carries a capillary which terminates in a platinum hook designed to hold the trabecula, as in [10]. The muscle bath during these experiments was an acetal-plastic plate with a through-hole which is enclosed with a cover slip on the top and bottom.

The displacement of the motor is measured using a heterodyne laser interferometer with resolution of 0.3 nm. Displacement estimates were used to close a position control loop based on a simple PID algorithm operating in the Labview Real-Time operating system.

C. Sarcomere Length Detection Algorithm

The image of the cardiac trabecula resulted in a 512 x 1024 array of 8-bit greyscale pixel information. The trabecula was oriented so that the Z-lines of the sarcomeres were approximately vertical with respect to the image. In the ideal case, each row of pixels would contain a "clear" image of some portion of a muscle cell, with a sinusoidal intensity profile, in which the period of the sinusoid corresponds to the separation of sarcomeres. In reality, it is often the case that the sarcomere information is partially obscured by a combination of occluding tissue fragments, and the fact that the myocytes through the tissue thickness are not in perfect alignment.

Each row of the image was Fourier-transformed within the FPGA. To reduce issues associated with the transform of non-periodic signals, we first windowed the data with a Hanning window. This had the effect of reducing the frequency noise associated with discontinuities at the start and end of the signal period. The resolution of the frequency spectrum bins is related to the camera pixel resolution by the following relationship:

$$df = \frac{1}{dxN} \tag{1}$$

where *df* is the frequency resolution, *dx* is the per-pixel spatial resolution, and N is the number of points making up the signal.

After transforming the pixel row information into the frequency domain, we performed a search for the maximum value over the range of frequencies corresponding to physically realistic sarcomere lengths. Given a sufficient signal strength (sufficient contrast/high alignment/low occlusion), this maximal value should correspond to the average sarcomere length along that image row. By interpolating the value of the maximal frequency bin and its adjacent bins, we can increase the frequency resolution significantly.

For the interpolation we used Grandke's method [11] as it is reported to be robust at low signal-to-noise ratios (SNR). Using Grandke's method, the maximum bin in the search region and the second largest (adjacent) bins were interpolated using the following equations:

$$\alpha = \frac{B}{A} \tag{2}$$

$$\delta = \frac{2\alpha - 1}{\alpha + 1} \tag{3}$$

where *A* is the maximum value, *B* is the value of the largest adjacent, and δ is the value of the deviation from the maximum bin, where the direction of deviation is dependent on the location of the largest adjacent (before or after the maximum). The deviation was then summed with the index of the maximum bin (i_{max}), and the sarcomere length calculated using:

$$SL = \frac{1}{(\delta + i_{max})df} \tag{4}$$

For the purposes of further discussion we define $(\delta + i_{max})$ as $I_{interpolated}$. The signal-to-noise ratio (SNR) was used to quantify the quality of the estimate. The SNR of each row was computed by integrating over the bins containing the maxima and its two adjacents, then dividing by the integral of the remaining bins in the search range. Rows with an SNR of less than a predefined threshold (SNR_T) were rejected. This approach reduced the influence of noisy rows on the final image estimate. The computed sarcomere lengths were then averaged to give an estimate for the sarcomere length in each image.

All sarcomere-length analysis computations were performed in the FPGA environment using software coded in LabVIEW 2011, with the FPGA and RealTime toolboxes (National Instruments). The FPGA software then made available all results to the LabVIEW Realime operating system for recording, and future implementation of sarcomere-length control.

D. Simulation of Noise Effects

To explore the effects of noise on the performance of the interpolation algorithm, a simulation study was performed in Matlab. A series of "noisy" test images (of known SNR) was generated. Each row in each test image consisted of a sinusoidal signal (period 2.0 µm, length 1024 points, unity amplitude) summed with a randomly-generated white-noise signal. The power of the noise signal was an integer multiple of the power of the sinusoid. A total of 49 images were generated, with SNR ranging from 0.04 to 1.

Each image was passed through the interpolation algorithm, resulting in estimates of the spatial period and SNR of each row. Spatial period estimates were averaged across all rows. The uncertainty of the estimated spatial period was quantified by the standard error in the mean of the row estimates. The mean absolute error for each image was determined from the difference between the mean estimated spatial period and the predetermined spatial period.

E. Calibration

To calibrate the sarcomere-length imaging and analysis system, images of a 1.667 μm pitch diffraction grating were acquired (Fig. 2). Each row in the image was processed by the interpolation algorithm, returning an estimate of $I_{interpolated}$, for that row. The average value of $I_{interpolated}$ was computed across all row-estimates. We then iteratively manipulated dx, until the inverse of the frequency at $I_{interpolated}$ matched the expected period. A spatial sampling rate of $1/dx = 0.00385$ pixels/nm resulted in an average spacing estimate of 1.667 μm with a standard deviation of 0.266 nm.

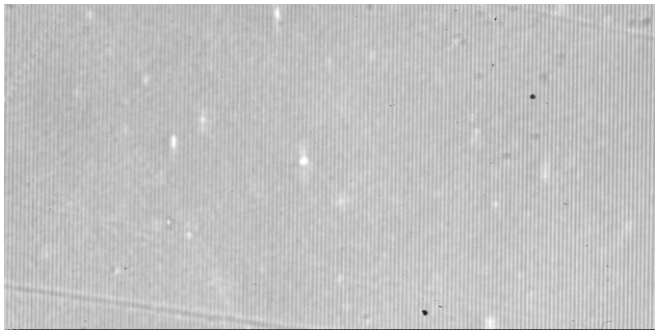

Figure 2: Image of a 600 lines per mm diffraction grating.

F. Experimental Design and Protocols

Wistar rats were anaesthetized using isofluorane prior to cervical-spinal dislocation, thoracotomy and cardiectomy (as approved by The University of Auckland Animal Ethics Committee). The excised heart was quickly plunged into cold dissection solution. The aorta was cannulated and the coronary vasculature was Langendorff-perfused with dissection solution, which contained (in mM): 130 NaCl, 6 KCl, 1 $MgCl_2$, 0.5 NaH_2PO_4, 0.3 $CaCl_2$, 10 HEPES, 10 glucose, and 20 BDM (2,3-butanedione monoxime), had a pH of 7.4 (adjusted using Tris) and was vigorously bubbled with 100% O_2, at 22 ºC - 23 ^{o}C. An unbranched and geometrically-uniform trabecula (diameter: 150 μm, length: 700 μm) was dissected from the right-ventricular inner wall.

The muscle bath was filled with BDM and the muscle was attached to the two platinum hooks at either end. The objective was focused and manipulated in the plane normal to the optical axis to obtain an image of the tissue which showed visible striations. If no striations were visible in an initial search, the motor was used to displace the hook in 25 μm increments until visible striations were observed. The height of the condenser with respect to the specimen, and the light-source intensity were then adjusted to achieve maximum contrast.

While recording at a rate of 2 Hz, the muscle was stretched in 25 μm increments under closed-loop control by the motor up to 125 μm, or the muscle separated from the hooks.

III. Results

The effect of noise on the efficacy of the interpolation algorithm, as determined by our simulation, is shown in Figure 3. As the SNR decreases below 0.09, both the mean absolute error and standard error of the estimate increase rapidly. For images of SNR ≥ 0.1, the standard error in the mean of the row estimates is less than 1 nm, and the mean absolute error is ≈ 2 nm. Consequently, SNR_T was assigned the value of 0.1 in all subsequent analyses.

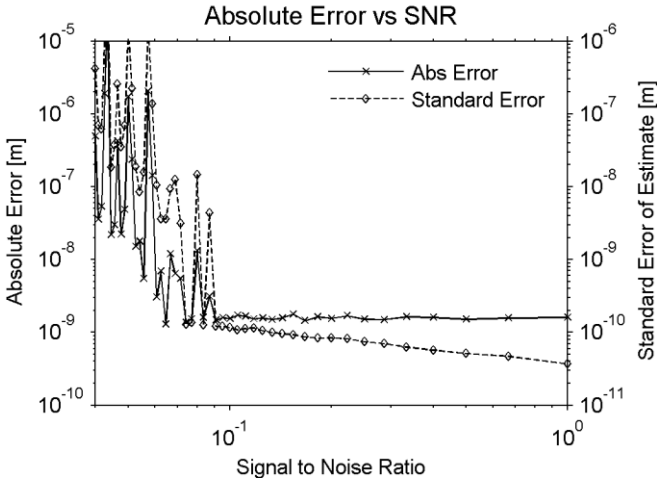

Figure 3 Absolute error and standard error versus signal to noise ratio

Figure 4 shows a typical image of a section of a cardiac trabecula. For this image our search algorithm returned a mean sarcomere-length estimate of 2.414 μm. The standard error of the mean of the valid row-by-row estimates of sarcomere length was 10 nm (computed over 186 valid rows).

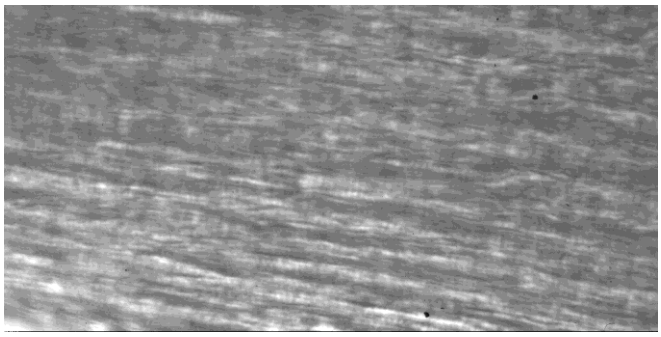

Figure 4: Typical image showing a section of cardiac trabecula

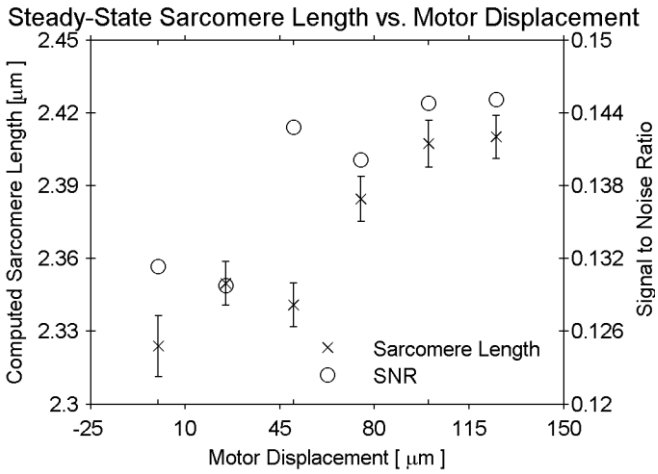

Figure 5 Mean estimated sarcomere length (bars indicate standard error) and SNR versus motor displacement

Figure 5 shows the estimated mean sarcomere length and associated signal to noise ratio, as a single relatively thin trabecula was stretched by 125 μm in 25 μm steps. The error bars represent the standard error of the valid row estimates.

IV. Discussion

The results of our simulation study (Figure 3) show that the interpolation algorithm performs well on rows with an SNR of 0.1 or greater. The absolute error in the estimated spatial period of these rows is < 2 nm. For SNR < 0.1, the standard error in the mean estimated sarcomere length is highly variable. Consequently, we reject estimates from lines with SNR < 0.1.

The results of our stretching experiment (Figure 5) show that the estimated sarcomere length increases with muscle length, as expected. The corresponding average SNR in the image is considerably greater than our threshold SNR_T (0.1). At the observed values of SNR, the expected standard error attributable to the algorithm alone is less than 1 nm. The relatively large observed standard error (~10 nm) of the row estimates is possibly indicative of a true variation in sarcomere length. It is unclear at this stage why the standard error of the steady-state estimates decreases with increasing sarcomere length. However, this phenomenon could be a consequence of structural reordering with increasing strain leading to improved image contrast.

As trabecula thickness increased beyond 150 μm, the performance of the algorithm degraded severely. The opacity of the central region in such muscles provided poor SNR, leaving only a thin region along the side of each muscle through which sufficient light passed to observe sarcomeres.

The white-noise model used in our simulation study may not accurately represent the noise spectrum of real images. We aim to improve our simulations by building a more accurate noise model based on experimental data in order to improve future simulations and hence our estimate of an appropriate threshold level.

In the future, we aim to explore the effect of discontinuities in sarcomere spacing along each row, and the variation of sarcomere length across each image. To achieve this, we will slide a window along each row, while quantifying the estimated sarcomere length in the window.

V. Conclusion

For sufficiently thin (<150 μm) trabeculae, our sarcomere length measurement system provided useful estimates of mean sarcomere length and sarcomere length distribution in isolated cardiac trabeculae. The computed results show an increase in mean sarcomere length with increasing stretch. Further investigation is required to determine whether the standard error of row-by-row measurements in our experiment is a fundamental property of cardiac trabeculae, or an artifact of our illumination and imaging system.

VI. Acknowledgments

The authors thank June-Chiew Han and Soyeon Goo for their assistance with obtaining and mounting muscle preparations.

References

[1] J. C. Han, *et al.*, "A unique micro-mechano-calorimeter for simultaneous measurement of heat rate and force production of cardiac trabeculae carneae," *J. App. Phys.*, vol. 107, pp. 946-951, Sep 2009.

[2] J. C. Han, *et al.*, "Radius-dependent Decline of Performance in Isolated Cardiac Muscle Does Not Reflect Inadequacy of Diffusive Oxygen Supply," *Am J Physiol Heart Circ Physiol,* vol. 300, pp. H1222-H1236, Jan 7 2011.

[3] A. Taberner, *et al.*, "Stress Development, Heat Production and Dynamic Modulus of Rat Isolated Cardiac Trabeculae Revealed in a Flow-Through Micro-mechano-calorimeter," in *Proceedings of the 32nd Ann. Int. Conf. of the IEEE EMBS*, Buenos Aires, Argentina, 2010.

[4] J. C. Han, *et al.*, "Energetics of stress production in isolated cardiac trabeculae from the rat," *Am J Physiol Heart Circ Physiol,* vol. 299, pp. H1382-H1394, 2010.

[5] A. J. Taberner, *et al.*, "A sensitive flow-through microcalorimeter for measuring the heat production of cardiac trabeculae," in *Proceedings of the 26th Ann. Int. Conf. of the IEEE EMBS, Vols 1-7*, San Francisco, 2004, pp. 2030-2033.

[6] A. J. Taberner, *et al.*, "Characterization of a flow-through microcalorimeter for measuring the heat production of cardiac trabeculae," *Review of Scientific Instruments,* vol. 76, pp. 104902-104908, 2005-10 2005.

[7] P. de Tombe and H. ter Keurs, "Force and Velocity of Sarcomere Shortening in Trabeculae From Rat Heart Effects of Temperature," *Circulation Research,* pp. 1239-1254, 1990.

[8] H. ter Keurs, *et al.*, "Tension development and sarcomere length in rat cardiac trabeculae. Evidence of length-dependent activation," *Circulation Research,* vol. 46, pp. 703-714, May 1, 1980 1980.

[9] K. P. Roos and a. J. Brady, "Individual sarcomere length determination from isolated cardiac cells using high-resolution optical microscopy and digital image processing.," *Biophysical journal,* vol. 40, pp. 233-244, 1982.

[10] J. C. Han, *et al.*, "A unique micromechanocalorimeter for simultaneous measurement of heat rate and force production of cardiac trabeculae carneae," *J Appl Physiol,* vol. 107, pp. 946-951, 2009.

[11] T. Grandke, "Interpolation Algorithms for Discrete Fourier Transforms of Weighted Signals," *Instrumentation and Measurement, IEEE Transactions on,* vol. 32, pp. 350-355, 1983.